IIETA International Information and Engineering Technology Association
Advancing the World of Information and Engineering

Journal of New Materials for Electrochemical Systems
Vol. 24., No. 3 July 2021, pp. 201-207
Journal homepage: http://iieta.org/journals/jnmes

Strontium Substituted $SmNiO_3$: Novel Electrode Materials for Alkaline Water Electrolysis

Reena Parihar, Priya Sharma, Amritpal Singh Chaddha, Narendra Kumar Singh*

Department of Chemistry, Faculty of Science, University of Lucknow, Lucknow-226007 (INDIA)

*Corresponding Author Email: nksbhu@yahoo.com, singh_narendra@lkouniv.ac.in, ORCID: 0000-0002-9108-6545
Mob: +91-9451949105

https://doi.org/10.14447/jnmes.v24i3.a08

Received: May 15-2021
Accepted: August 10-2021

Keywords: *Samarium nickelates, sol-gel method, XRD, oxygen evolution, thermodynamic parameters*

ABSTRACT

Sr-substituted $SmNiO_3$ perovskite-type oxides have been investigated for their electrocatalytic properties towards oxygen evolution reaction (OER) in alkaline medium. Materials were obtained by using low temperature malic acid sol-gel route. To know the redox behaviour, electrocatalytic activity and thermodynamic parameters of oxides, cyclic voltammetry (CV) and anodic polarization curve (Tafel plot) were recorded in 1 M KOH at 25 ºC. X-ray diffraction (XRD) study indicates the formation of almost pure perovskite phase of the material. A pair of redox peaks was observed (anodic; Ep_a = 494±12 mV and corresponding cathodic; Ep_c = 360±4 mV) in the potential region 0.0-0.7 V prior to onset of OER. As observed in the case of La-based perovskite oxides, Sr-substitutions in the $SmNiO_3$ also enhance the electrocatalytic properties of the material. However, Sm-based oxides showed least electrocatalytic activity as compared to La-based oxides. The estimated values of Tafel slope and reaction order indicate that each oxide electrode, except $SmNiO_3$, follows similar mechanistic path towards OER. Standard entropy of activation ($\Delta S^{\circ\#}$), standard enthalpy of activation ($\Delta H^{\circ\#}$) and standard electrochemical energy of activation ($\Delta H_{el}^{\circ\#}$) was determined by recording the anodic polarization curve in 1M KOH at different temperatures.

1. INTRODUCTION

Perovskite-type mixed oxides of lanthanum having composition $La_{1-x}M_xM'O_3$ (where, M = Sr, Pb, Cu, Cr; M′ = Co, Mn, Ni and $0.0 \le x \le 0.8$) are considered as very promising materials and have been extensively studied for oxygen evolution/reduction reaction [1-30]. These materials have several technological applications [1,31,32]. There are several methods employed to synthesize these oxides. These include, high temperature solid state reaction and thermal decomposition methods [33-38], which generally produced oxides with low specific surface area and reduced homogeneity and low temperature methods [39-43] in which amorphous organic acids, like malic acid (MA), citric acid (CA), polyacrylic acid (PAA), citric acid-ethylene diamine (CA-EDA), polyvinylpyrrolidone (PVP) etc are used as precursors. These low temperature methods facilitate to provide homogeneity in the metal ions and produced oxides with high specific surface area and therefore improved electrochemical properties.

Recently, Azad et al. [44] reported oxygen evolution electrocatalytic properties of some perovskite mixed oxides as bifunctional electrocatalysts with current density 10 mA cm^{-2} at E = 1.65 V vs RHE. Sczancoski et al. [45] developed Fe-doped $LaNiO_3$ electrocatalysts for OER studies at deposited pyrolytic graphite sheets and found highest activity with $LaNi_{0.4}Fe_{0.6}O_3$ having Tafel slope value of 52 mV $decade^{-1}$. Findings of these literatures revealed that the metal ios have vital role in the enhancement of physical and electrocatalytic properties of materials. Further, it has been observed that most of the OER studies have been carried out with La-based perovskite oxides. Sm-based perovskites are very little investigated with regards to oxygen evolution/reduction reaction.

Shao-Horn et al. [46] used elements of lanthanide series instead of lanthanum and prepared double perovskites $(Ln_{0.5}Ba_{0.5})CoO_{3-\delta}$ (Ln = Pr, Sm, Gd and Ho) by adopting thermal decomposition method. They observed better electrocatalytic activity towards oxygen evolution reaction in alkaline solution. Very recently [27], we found better results towards OER with partial substitution of Sm for Sr in $La_{0.4}Sr_{0.6}CoO_3$.

In view of the above, we extended our research and used Sm-element instead of La to obtain perovskite-type oxides and further studied their electrocatalytic properties for OER in alkaline medium. Results, so obtained, are described in this paper.

2. EXPERIMENTAL

Strontium substituted $SmNiO_3$ having compositions $Sm_{1-x}Sr_xNiO_3$ ($0 \le x \le 0.8$) were prepared by adopting the method reported by Teraoka et al. [41]. In each preparation, all the reagents and chemicals were taken in purified form. The stoichiometric amount of metal nitrates and excess amount of malic acid were dissolved in 500 ml double distilled. 35%

ammonia solution was used to maintain the pH of mixture 3.5, which then concentrated over a water bath at 60-70°C. A gel like mass was obtained which decomposed and sintered at 600°C for 5h to get the desired oxide material. Techniques like, X-ray diffractometer (Philips and Panalytical Powder X-Ray Diffractometer) provided with radiation source Cu-Kα (λ = 1.54056 Å) and Scanning Electron Microscope (JEOL, JSM 6490) were used to determine the phase and morphology of the materials. The crystallite size of the material was calculated by using Scherer's formula.

The electrocatalytic property of the material was determined in the form of oxide film electrode on pre-treated Ni-support. The procedure adopted for the treatment of Ni-support, preparation of oxide film and electrical contact was same as described elsewhere [9,15]. During experiment, the oxide film electrode was used as working electrode. Hg/HgO /1M KOH and Pt-foil were used as reference and auxiliary electrode, respectively. A three-electrode single compartment glass cell, which is connected to the potentiostat/galvanostat (Gamry Reference 600 ZRA) and corrosion and physical electrochemical software compiled personal computer, was used for the electrochemical studies. In order to minimise the additional potential drop, the reference electrode was connected electrically to the electrolyte (1M KOH) via a Luggin capillary (KCl/Agar-Agar salt bridge).

3. RESULTS AND DISCUSSION

3.1 X-Ray Diffraction (XRD)

X-ray diffraction (XRD) patterns of oxide powders, $Sm_{0.2}Sr_{0.8}NiO_3$ and $Sm_{0.6}Sr_{0.4}NiO_3$, sintered at 600 ºC for 5h and recorded between 2θ = 20° to 100° are shown in Fig. 1. The observed patterns indicates the formation of almost perovskite phase of the material and found to be very similar to those with Sm-substituted La(Sr)CoO_3 [27] obtained by PVP method, which followed hexagonal crystal geometry of respective JCPDS ASTM file 25-1060. The crystallite size was calculated by using Scherer's formula [47] and found to be ~30 and ~40 nm for $Sm_{0.2}Sr_{0.8}NiO_3$ and $Sm_{0.6}Sr_{0.4}NiO_3$, repesctvely.

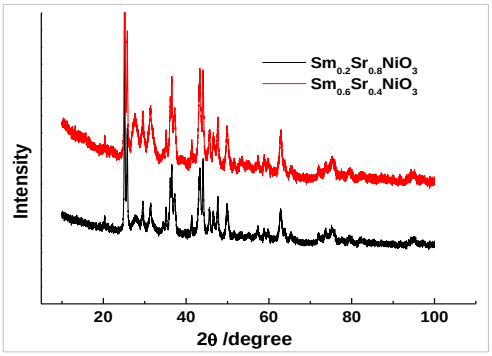

Figure 1: XRD powder patterns of oxides sintered at 600°C for 5 h

3.2 Scanning Electron Micrograph (SEM)

Figure 2 represents the SE-micrograph of sintered (600°C for 5 hrs) $SmNiO_3$ and $Sm_{0.2}Sr_{0.8}NiO_3$ oxide powder at the magnification ×200. Morphological appearance of both oxides are seemed to be similar and showed nebulous structure. Some small pores has also been observed in the oxide matrix.

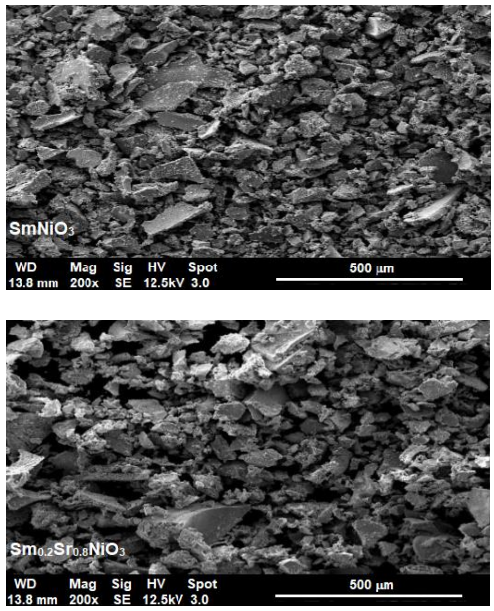

Figure 2: SE Micrographs of oxide powder sintered at 600°C for 5 hrs.

3.3 Cyclic Voltammetry (CV)

Figure 3 represents cyclic voltammogram of the oxide film electrode on Ni-substrate between potential region 0.0-0.7 V in 1M KOH at 25°C (scan rate = 20 $mVsec^{-1}$). Each voltammogram revealed a pair of redox peak, an anodic (Ep_a = 494 ± 12 mV) and corresponding cathodic (Ep_c=360 ± 4 mV), prior to the onset of oxygen evolution reaction. The peak potential values of each voltammetric curve (Table 1) corresponds to that obtained with the bare Ni [48]. Further, the CV of the oxide on Pt-substrates did not exhibit any redox peaks under similar experimental conditions. This specifies that the redox peaks might be due to the oxidation-reduction of Ni-substrate, which comes into contact with electrolyte during the cycle process through pores, cracks and grain boundaries. Aslo, it has been reported [49] that perovskite oxides prepared at low temperature are highly hygroscopic and may undergo hydration in electrolytic solution.

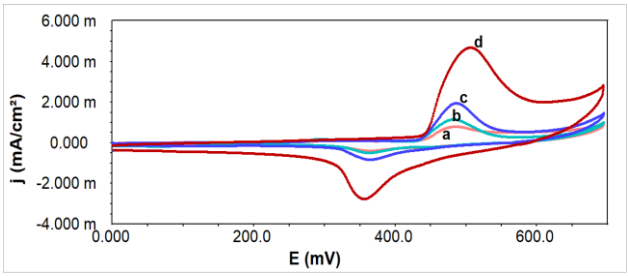

Figure 3: Cyclic voltammograms of Ni/ Sm1-xSrxCoO3 ($0 \leq x \leq 0.8$) in 1M KOH at 25˚C; (scan rate = 20 mV sec^{-1}); a: $SmNiO_3$, b: $Sm_{0.8}Sr_{0.2}NiO_3$, c: $Sm_{0.6}Sr_{0.4}NiO_3$, d: $Sm_{0.2}Sr_{0.8}NiO_3$

Other voltammetric constituents, such as peak separation potential ($\Delta E_p = E_{Pa} - E_{Pc}$), formal redox potentail [$E° = (E_{Pa} - E_{Pc})/2$], anodic and cathodic peak current, volatmmetric charge (q), etc were estimated from the voltammetric curve and listed in Table 1. With exception to $Sm_{0.2}Sr_{0.8}NiO_3$, the value of ΔE_p was almost same with each oxide electrode. A negligible change in the formal redox potential has been observed with the substitution of Sr for Sm in the base oxide ($SmNiO_3$). Anodic peak current, cathodic peak current and voltametric charge (q) are increased with increase in concentration of Sr in the oxide. The value of q is estimated by integrating the CV curve from zero to the potential just prior the OER. The ratio of anodic and cathodic peak current is more than unity, indicating the irreversibility [50-52] of the redox process.

Table 1: Values of the cyclic voltammetric parameters of Ni/ $Sm_{1-x}Sr_xNiO_3$ ($0 \leq x \leq 0.8$) in 1 M KOH at 25 °C (scan rate = 20 mV sec^{-1})

Electrode	E_{Pa} /mV	E_{Pc} /mV	ΔE_p /mV	E°/ mV	$\lvert j_{pa} \rvert$ /mA cm^{-2}	$\lvert j_{pc} \rvert$ /mA cm^{-2}	$\frac{\lvert j_{pa} \rvert}{\lvert j_{pc} \rvert}$	q /mC cm^{-2}
$SmNiO_3$	483	360	123	422	0.78	0.35	2.2	1.7
$Sm_{0.8}Sr_{0.2}NiO_3$	482	362	120	422	1.14	0.52	2.2	2.6
$Sm_{0.6}Sr_{0.4}NiO_3$	486	364	122	425	1.94	0.84	2.3	3.7
$Sm_{0.2}Sr_{0.8}NiO_3$	506	356	150	431	4.69	2.77	1.7	16.0

The effect of scan rate on the redox process has also been studied in 1M KOH at 25°C and shown in Fig. 4 for the $Ni/Sm_{0.2}Sr_{0.8}NiO_3$. The nature of CV curve as shown figure 4 is almost similar to that observed at scan rate of 20 mV sec^{-1}. But, a shift in anodic and cathodic peak potential was observed with the increase of scan rates from 20 to 120 mV sec^{-1}.

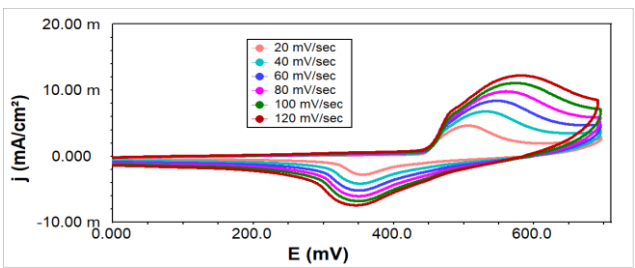

Figure 4: Cyclic voltammogram of $Ni/Sm_{0.2}Sr_{0.8}NiO_3$ film electrode at different scan rates in 1M KOH (25˚C)

It is found that both anodic and cathodic peak currents increased linearly with increase in the scan rates. The variation is represented in the plot of $\lvert j_P \rvert$ vs square root of scan rate (Fig. 5) for $Sm_{0.2}Sr_{0.8}NiO_3$ oxide electrode. The voltammetric charge (q) was also plotted against $(\text{scan rate})^{-1/2}$ and shown in Fig. 6. The straight line obtained indicates that the surface redox behaviour is diffusion controlled [15].

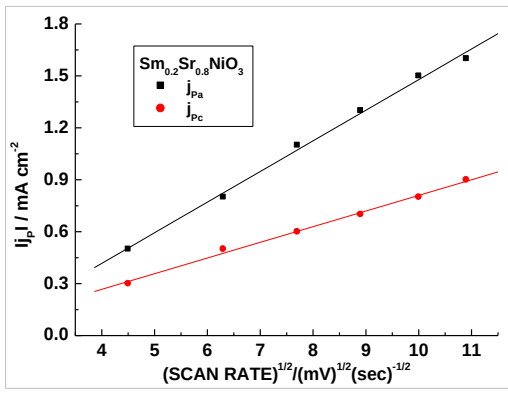

Figure 5: Plot of $|j_P|$ vs $(\text{scan rate})^{1/2}$ for the oxide film electrode on Ni in 1M KOH (25 °C)

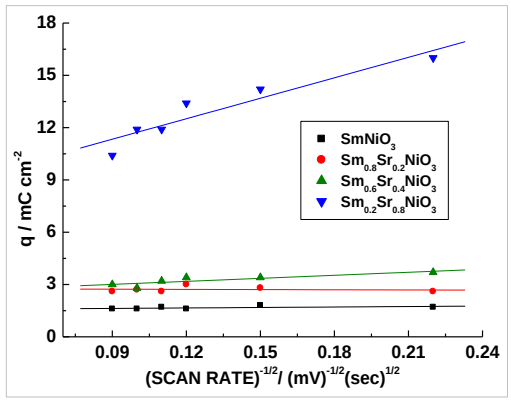

Figure 6: Plot of voltammetric charge (q) vs $(\text{scan rate})^{-1/2}$ for the oxide film electrode on Ni in 1M KOH (25 °C)

3.4 Electrocatalytic Activity

To know the electrocatalytic activity of the oxide electrocatalyst, iR-compensated anodic polarization curves (E vs.log j) was recorded in 1M KOH at 25 °C. The polarization curve, so obtained is shown in Fig. 7. The Tafel slope values as well as the electrocatalytic activity in terms of potential and current density were estimated from the polarization curve and listed in Table 2.. The Tafel slope value were ranged between 111-118 $mVdecade^{-1}$. On the comparison of electrocatalytic activity in terms of current density at fixed potential of 800 mV, it is observed that a slight increase in the electrocatalytic activity has been found with Sr-substitution. The activity being maximum with 0.8 mol Sr-substitution.

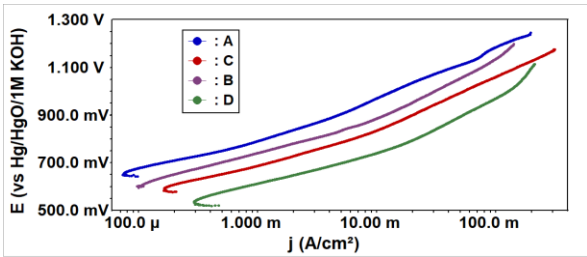

Figure 7: Tafel plots for oxygen evolution on $Ni/Sm_{1-x}Sr_xNiO_3$ ($0 \leq x \leq 0.8$) in 1M KOH at 25 ˚C (scan rate: 0.2 $mVsec^{-1}$).
A: $SmNiO_3$, B: $Sm_{0.8}Sr_{0.2}NiO_3$, C: $Sm_{0.6}Sr_{0.4}NiO_3$,
D: $Sm_{0.2}Sr_{0.8}NiO_3$

Table 2: Electrode kinetic parameters for oxygen evolution reaction on $Ni/Sm_{1-x}Sr_xNiO_3$ ($0 \leq x \leq 0.8$) electrodes in 1 M KOH at 25°C

Electrode	Tafel slope (b)	Order (p)	E/ mV at j/ mA cm^{-2}		j/ mA cm^{-2} at E/ mV	
			10	100	700	800
$SmNiO_3$	118	1.9	921	1134	0.5	1.1
$Sm_{0.8}Sr_{0.2}NiO_3$	113	1.2	849	1068	0.9	1.5
$Sm_{0.6}Sr_{0.4}NiO_3$	114	0.9	888	1116	0.9	1.3
$Sm_{0.2}Sr_{0.8}NiO_3$	111	1.0	815	1045	1.2	4.1

As per Table 2, oxide electrodes show the following order of electrocatalytic activity at constant potential (E = 800 mV);

$Sm_{0.2}Sr_{0.8}NiO_3$ (j = 4.1 mA cm^{-2}) > $Sm_{0.8}Sr_{0.2}NiO_3$ (j = 1.5 mA cm^{-2}) > $Sm_{0.6}Sr_{0.4}NiO_3$ (j = 1.3 mA cm^{-2}) > $SmNiO_3$ (j = 1.1 mA cm^{-2})

The anodic polarization curve was recorded to determine the reaction order of OE with each oxide electrode in different KOH concentraation at 25°C. During the process, the electrical intensity of the each electrolytic solution was kept uniform. An inert electrolyte KNO_3 was used to maintain the ionic strength (µ = 1.5) of each solution constant. A representative polarization curve for $Ni/Sm_{0.2}Sr_{0.8}NiO_3$ is shown in the Fig. 8. From figure, values of current density (log j/ A cm^{-2}) were estimated at a certain potential and plotted against log [OH^-] , which is shown in the Fig. 9 at a constant potential of E=700 mV. The order of reaction was calculated by measuring the slope of straight line and values are listed in Table 2. The observed values of Tafel slope and reaction order as given in Table 2 suggest that the OER taking place at the electrocatalysts follows similar mechanistic path except $SmNiO_3$, which has reaction order 1.9 with Tafel slope 118 mV $decade^{-1}$.

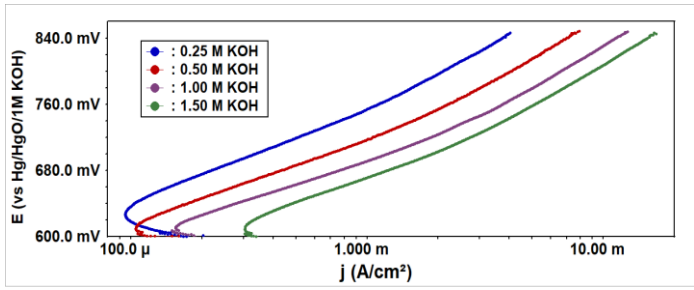

Figure 8: Tafel plots for oxygen evolution on $Ni/Sm_{0.2}Sr_{0.8}NiO_3$ at varying KOH concentrations (µ = 1.5) at 25 ˚C

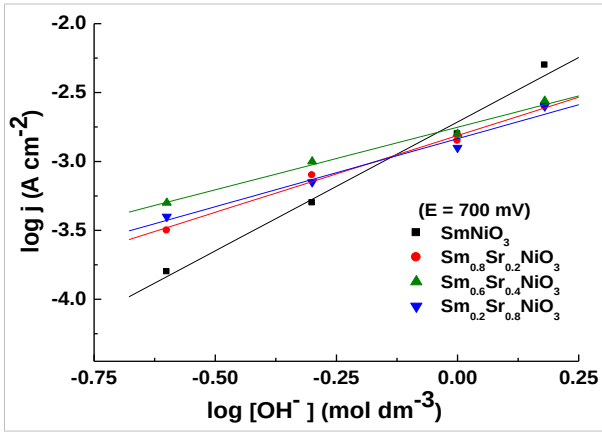

Figure 9: Plot of log j vs log [OH^-] for $Ni/Sm_{1-x}Sr_xNiO_3$ ($0 \leq x \leq 0.8$) electrodes.

3.5 Thermodynamic Parameters

Thermodynamic parameters of two oxide electrocatalysts towards OER have also been determined by recording the anodic polarization curve in 1 M KOH at 20, 30, 40, and 50°C. A set of polarization curve for $SmNiO_3$ is shown in Figure 10. During the experiment, the temperature of the reference electrode was kept constant. From figure, values of log j (in mA cm^{-2}) were estimated at a constant applied potential and plotted against 1/T. The standard apparent enthalpy of activation ($\Delta H_{el}^{\circ\#}$) was calculated at a certain potential (E = 650 mV) by measuring the slope of Arrhenius plot, log j vs 1/T (Fig. 11).

Further, following two relations (1) and (2) [53] are used to determine the values of standard enthalpy of activation ($\Delta H^{\circ\neq}$) and standard entropy of activation ($\Delta S^{\circ\neq}$), respectively.

$$\Delta H_{el}^{\circ\neq} = \Delta H^{\circ\neq} - \alpha F\eta \qquad \ldots\ldots (1)$$

$$\Delta S^{\circ\neq} = 2.3R\left[\log j + \frac{\Delta H_{el}^{\circ\neq}}{2.3RT} - \log (nF\omega C_{OH^-})\right] \qquad \ldots\ldots (2)$$

In equation (1), α (= 2.303RT/bF) is the transfer coefficient. η is the overpotential equal to E - E_{O2/OH^-}, where E is the potential applied and E_{O2/OH^-} (= 0.303 V vs. Hg/HgO) [54] is the theoretical equilibrium Nernst potential in 1 M KOH at 25 ˚C. The Tafel slope (b) is determined from the polarization curves obtained at different temperatures. R, F are the universal constants and T is the absolute temperature.

In equation (2), the value of frequency term (ω) is equal to k_BT/h. k_B and h are the Boltzmann constant and Planck's constant, respectively. Here, the value of 'n' was taken 2 in every calculation. The calculated values of thermodynamic parameters are listed in the Table 3. Values of electrochemical activation energy were found to be 47.5 and 54.9 kJ mol^{-1} for $SmNiO_3$ and $Sm_{0.8}Sr_{0.2}NiO_3$, respectively.

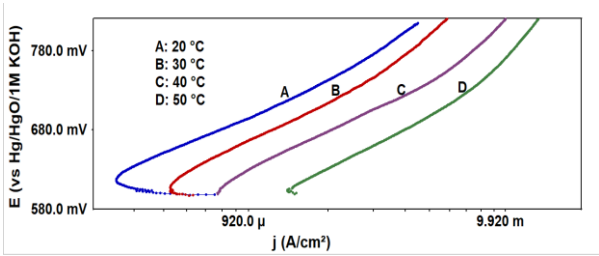

Figure 10: Anodic polarization curve for the $SmNiO_3$ film electrode on Ni at different temperatures in 1 M KOH

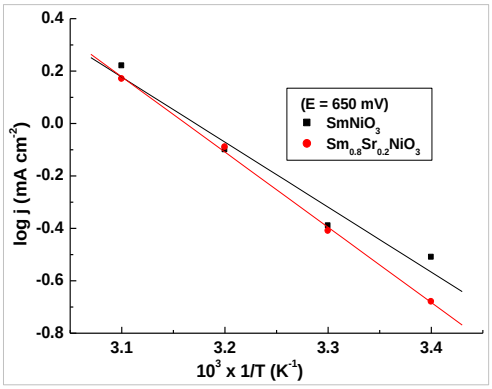

Figure 11: The Arrhenius plot at a constant applied potential (650 mV) for La1-xSrxCoO3 (x = 0 and 0.2) in 1 M KOH

Table 3: Thermodynamic parameters for O_2 evolution on $Ni/Sm_{1-x}Sr_xNiO_3$ (x = 0 and 0.2) in 1 M KOH

Electrode	$\Delta H_{el}^{\circ\#}$ (kJ mol^{-1})	$-\Delta S^{\circ\#}$ ($Jdeg^{-1}$ mol^{-1})	α	$\Delta H^{\circ\#}$ (kJ mol^{-1})
$SmNiO_3$	47.5	195.1	0.5	64.4
$Sm_{0.8}Sr_{0.2}NiO_3$	54.9	171.9	0.5	71.5

CONCLUSION

The present work has been undertaken to study the electrocatalytic properties of Sm-based perovskite over La-based. Sr-substitution in the base oxide increased the electrocatalytic properties of the material. But, this increase is not so significant as observed in the case of La-based perovkites. As per present study, Sm-based perovskites are not prolific electrocatalysts for the electrolysis point of view.

ACKNOWLEDGEMENTS

Authors are thankful to SERB (DST), New Delhi for providing electrochemical impedance system under Fast Track Scheme for Young Scientist (No.: SR/FT/CS-044/2009). Thanks are also given to BSIP and Department of Chemistry, University of Lucknow for SEM and basic infrastructure, respectively.

REFERENCES

1. Meadocroft D. B. (1970). Low-cost oxygen electrode material, Nature, 226:847-848. https://doi.org/10.1038/226847a0.
2. Matsumoto Y., Sato E. (1979). Oxygen evolution on $La_{1-x}Sr_xMnO_3$ electrodes in alkaline solutions, Electrochim. Acta, 24:421-423. https://doi.org/10.1016/0013-4686(79)87030-9.
3. Matsumoto Y., Yamada S., Nishida T., Sato E. (1980). Oxygen evolution on $La_{1-x}Sr_xFe_{1-y}Co_yO_3$ series oxides, J. Electrochem. Soc., 127:2360-2364. https://doi.org/10.1149/1. 2129415.
4. Yamada S., Matsumoto Y., Sato E. (1981). Oxygen Evolution on $La_{1-x}Sr_xFe_{1-y}Ni_yO_3$ Series Oxides, The journal of the Electrochemical Society of Japan, 49:269-273. https://doi.org/10.5796/kogyobutsurikagaku.49.269
5. Kobussen A.G.C., Willems H., Broers G.H.J. (1982). The oxygen evolution on $La_{0.5}Ba_{0.5}CoO_3$: Passivation processes, J. Electroanalytical Chemistry and Interfacial Electrochemistry 142:85-94. https://doi.org/10.1016/S0022-0728(82)80007-7
6. Bockris J. O'M, Otagawa T., Young V. (1983). Solid state surface studies of the electrocatalysis of oxygen evolution on perovskites, J. Electroanal. Chem., 150:633-643. https://doi.org/10.1016/S0022-0728(83)80243-5.
7. Shimizu Y., Matsuda H., Miura N., Yamazoe N. (1992). Bi-functional Oxygen Electrode Using Large Surface Area Perovskite-type Oxide Catalyst for Rechargeable Metal-Air Batteries, Chem. Lett., 21:1033-1036. https://doi.org/10.1246/cl.1992.1033.
8. Schmidt T., Wendt H. (1994). Electrocatalysis of cathodic hydrogen and anodic oxygen evolution in alkaline water electrolysis by in situ activation procedures, Electrochim. Acta., 39:1763-1767. https://doi.org/10.1016/00134686(94)85162-X.
9. Tiwari S. K., Chartier P., Singh R. N.(1995). Preparation of Perovskite-Type Oxides of Cobalt by the Malic Acid Aided Process and Their Electrocatalytic Surface Properties in Relation to Oxygen Evolution, J. Electrochem. Soc., 143:148-153. https://doi.org/10.1149/1.2043854.
10. Jain A. N., Tiwari S. K., Singh R. N. Chartier P. (1995). Low-temperature synthesis of perovskite-type oxides of lanthanum and cobalt and their electrocatalytic properties for oxygen evolution in alkaline solutions, J. Chem. Soc. Faraday Trans., 91:1871-1875. https://doi.org/10.1039/FT9959101871.
11. Singh R. N., Bahadur L., Pandey J. P., Singh S. P., Chartier P., Poillerat G. (1994). Preparation and characterization of thin films of $LaNiO_3$ for anode application in alkaline water electrolysis, J. Appl. Electrochem., 24:149-156. https://doi.org/10.1007/BF00247787.
12. Singh S. P., Singh R. N., Poillerat G., Chartier P. (1995), Physicochemical and electrochemical characterization of active films of $LaNiO_3$ for use as anode in alkaline water electrolysis, Int. J. Hydrogen Energy, 20:203-210. https://doi.org/10.1016/0360-3199(94)E0027-V.
13. Singh R. N., Jain A. N., Tiwari S. K., Poillerat G., Chartier P. (1995). Physicochemical and electrocatalytic properties

of $LaNiO_3$ prepared by a low-temperature route for anode application in alkaline water electrolysis., *J. Appl. Electrochem*., 25:1133-1138. https://doi.org/10.1007/BF00242541.

14. Tiwari S. K., Koenig J. F., Poillerat G., Chartier P., Singh R. N. (1998). Electrocatalysis of oxygen evolution/ reductionon $LaNiO_3$ prepared by a novel malic acid-aided method, J. Appl. Electrochem., 28:114-119. https://doi.org/10.1023/A:1003214321780.
15. Singh R. N., Tiwari S. K., Singh S. P., Singh N. K., Poillearat G., Chartier P. (1996). Synthesis of (La, Sr)CoO_3 perovskite films via a sol–gel route and their physicochemical and electrochemical surface characterization for anode application in alkaline water electrolysis, J. Chem. Soc. Faraday Trans., 92(14):2593-2597. https://doi.org/10.1039/FT9969202593.
16. Singh R. N., Tiwari S. K., Singh S. P., Jain A. N., Singh N. K. (1997). Electrocatalytic activity of high specific surface area perovskite-type $LaNiO_3$ via sol-gel route for electrolytic oxygen evolution in alkaline solution, Int. J. Hydrogen Energy, 22:557-562. https://doi.org/10.1016/S0360-3199(96)00176-0.
17. Sharma T., Singh N. K., Tiwari S. K., Singh R. N. (1998). Electrocatalytic properties of La-manganites prepared by low temperature synthesis, Ind. J. Engg. & Mat. Sci., 5:38-42.
18. Singh N. K., Tiwari S. K., Singh R. N. (1998). Electrocatalytic properties of lanthanum manganites obtained by a novel malic acid-aided route, Int. J. Hydrogen Energy, 23:775-780. https://doi.org/10.1016/S0360-3199(97)00119-5.
19. Lal B., Singh N. K., Singh R. N. (2001). Electrocatalytic properties of Sr-doped $LaMnO_3$ obtained by a new sol-gel route in relation to O_2 evolution in alkaline solution, Ind. J. Chem., 40 A:1269-1276.
20. Singh N. K., Lal B., Singh R. N. (2002). Electrocatalytic properties of perovskite-type $La_{1-x}Sr_xMnO_3$ obtained by a novel sol–gel route for O_2 evolution in KOH solutions, *Int.* J. Hydrogen Energy, 27:885-893. https://doi.org/10.1016/S0360-3199(02)00008-3.
21. Lal B., Raghunanda M. K., Gupta M., Singh R. N. (2005). Electrocatalytic properties of $La_{1-x}Sr_xCoO_3(0 \leq x \leq 0.4)$ perovskite-type obtained by a novel stearic acid sol–gel method for electrocatalysis of O_2 evolution in KOH solutions *Int. J. Hydrogen Energy*, 30:723-729. https://doi.org/10.1016/j.ijhydene.2004.07.002.
22. Suntivich J., Gasteiger H. A., Yabuuchi N., Nakanish H., Goodenough J. B., Shao-Horn Y. (2011). Design principles for oxygen-reduction activity on perovskite oxide catalysts for fuel cells and metal–air batteries, Nature Chemistry, 3:546-550. https://doi.org/10.1038/nchem.1069
23. Sunarso J., Torriero A. A. J., Zhou W., Howlett P. C., Forsyth M. (2012). Oxygen Reduction Reaction Activity of La-Based Perovskite Oxides in Alkaline Medium: A Thin-Film Rotating Ring-Disk Electrode Study, J. Phys. Chem., 116:5827-5834. https://doi.org/10.1021/jp211946n.
24. Yadav M. K., Yadav Ritu, Sharma Priya, Singh N. K. (2016). Synthesis and electrocatalytic properties of $La_{1-x}Sr_xCoO_3$ $(0 \leq x \leq 0.8)$ film electrodes for oxygen evolution in alkaline solutions, Int. J. Electrochem. Sci., 11:8633-8645. doi: 10.20964/2016.10.01.
25. Singh N. K., Yadav M. K., Fernandez C. (2017). Electrocatalytic properties of $La_{1-x}Cu_xCoO_3$ $(0 \leq X \leq 0.8)$ film electrodes prepared by malic acid sol-gel method at pH =3.75, Int. J. Electrochem Sci., 12:7128-7141. doi: 10.20964/2017.08.68.
26. Singh N. K., Sharma P., Kumar I., Chaddha A. S. (2019). Oxygen evolution electrocatalytic properties of perovskite-type $La_{1-x}Sr_xCoO_3$ $(0 \leq x \leq 0.8)$ oxides obtained by polyvinylpyrrolidone sol-gel route, Int. J. Electrochem. Sci., 14:11379-11390. doi: 10.20964/2019.12.70.
27. Singh N. K., Sharma P., Yadav M. K., Parihar R. (2020). Oxygen evolution electrocatalytic properties of perovskite-type oxides obtained by PVP sol-gel route: Part II. The effect of partial substitution of Sm for Sr in $La_{0.4}Sr_{0.6}CoO_3$, Int. J. Electrochem. Sci., 15:7001-7012. doi:10.20964/2020.07.81.
28. Shin Boyoon, Choi Sangwon, Tak Yongsug (2016). Electrocatalytic Activity of Co-based Perovskite Oxides for Oxygen Reduction and Evolution Reactions, *Int. J. Electrochem. Sci*., 11:5900-5908, https://doi.org/10.20964/2016.07.68.
29. Zhang Z., Zhou D., Wu X., Bao X., Liao J., Wen M. 2019). Synthesis of $La_{0.2}Sr_{0.8}CoO_3$ and its electrocatalytic activity for oxygen evolution reaction in alkaline solution, *Int. J. Hydrogen Energy*, 44:7222-7227, https://doi.org/10.1016/j.ijhydene.2019.01.268
30. Singh R. N., Lal B. (2002). High surface area lanthanum cobaltate and its A and B sites substituted derivatives for electrocatalysis of O_2 evolution in alkaline solution, *Int. J. Hydrogen Energy*, 27:445-46, https://doi.org/10.1016/S0360-3199(01)00078-7
31. Tseung A. C. C., Bevan H. L. (1973). A reversible oxygen electrode, J. Electroanal. Chem., 45:429-438. https://doi.org/10.1016/S0022-0728(73)80053-1.
32. Matsuki K., Kamada H. (1985). Research on Energy Conversion and Storage Through Chemical Process, SPEY, vol. 13 p. 181.
33. Bockris J. O. M., Otagawa T. (1984). The Electrocatalysis of oxygen evolution on perovskites, J. Electrochem. Soc., 131: 290-302. https://doi.org/10.1149/1.2115565.
34. Balej J. (1985). Electrocatalysts for oxygen evolution in advanced water electrolysis, Int. J. Hydrogen Energy, 10:89-99. https://doi.org/10.1016/0360-3199(85)90041-2.
35. Kobussen A. G. C., Buren van F. R., Den Belt van T. G. M., Wees van H. J. A. (1979). Oxygen evolution on $LaCoO_3$-type electrodes, *J. Electroanal Chem*., 96:123-125.
36. Matsumoto Y., Manabe H., Sato E. (1980). Oxygen evolution on $La_{1-x}Sr_xCoO_3$ electrodes in alkaline solutions, J. Electrochem Soc. 127:811-814. https://doi.org/10.1149/1.2129762
37. Wendt H., Plzak V. (1983). Electrocatalytic and thermal activation of anodic oxygen- and cathodic hydrogen-evolution in alkaline water electrolysis, Electrochim Acta, 28:27-34. https://doi.org/10.1016/0013-4686(83)85083-X.
38. Fiori G., Mari C. M. (1982). Electrocatalysis of oxygen evolution, Int. J. Hydrogen Energy, 7:489-493. https://doi.org/10.1016/0360-3199(82)90106-9.
39. Vidyasagar K., Gopalkrishnan J., Rao C.N.R. (1985). Synthesis of complex metal oxides using hydroxide, cyanide, and nitrate solid solution precursors, J. Solid state chem., 58:29-37. https://doi.org/10.1016/0022-4596(85)90266-x
40. Vassiliou J. K., Hornbostel M., Ziebarth R., Disalvo F. J. (1989). Synthesis and properties of $NdNiO_3$ prepared by

low-temperature methods, J. Solid State Chem., 81:208-216. https://doi.org/10.1016/0022-4596(89)90008-X
41. Teraoka Y., Kakebayashi H., Moriguchi I., Kagawa S. (1991). Hydroxy acid-aided synthesis of perovskite-type oxides of cobalt and manganese, Chemistry Letters, 20:673-676. https://doi.org/10.1246/cl.1991.673
42. Taguchi H., Yoshioka H., Matsuda D., Nagao M. (1993). Crystal structure of $LaMnO_{3+\delta}$ synthesized using poly (acrylic acid), Solid State Chem., 104:460-463. https://doi.org/10.1006/jssc.1993.1181.
43. Nagai T., Fujiwara N., Asahi M., Yamazaki Shin-Ichi, Siroma Z., Ioroi T. (2014). Synthesis of nano-sized perovskite-type oxide with the use of polyvinyl pyrrolidone, J. Asian Ceramic Society, 2:329-332. https://doi.org/10.1016/j.jascer.2014.08.004
44. Azad Uday Pratap, Singh Monika, Ghosh Sourav, Singh Ashish Kumar, Ganesan Vellaichamy, Singh Akhilesh Kumar, Prakash Rajiv (2018). Facile synthesis of BSCF perovskite oxide as an efficient bifunctional oxygen electrocatalyst, Int. J. Hydrogen Energy, 43:20671-20679. https://doi.org/10.1016/j.ijhydene.2018.09.134
45. Gozzo C. B., Mario R. S. Soares, Sczancoski J. C., Nogueira I. C. , Edson R. Leite. (2019). Investigation of the electrocatalytic performance for oxygen evolution reaction of Fe-doped lanthanum nickelate deposited on pyrolytic graphite sheets *Int. J. Hydrogen Energy,* 39:21659-21672. https://doi.org/10.1016/j.ijhydene.2019.06.109
46. Grimaud Alexis, May Kevin J., Carlton Christopher E., Lee Yueh-Lin, Risch Marcel, Hong Wesley T., Zhou Jigang, Shao-Horn Y. (2013). Double perovskites as a family of highly active catalysts for oxygen evolution in alkaline solution, Nature Communications, 4:1-7. https://doi.org/10.1038/ncomms3439.
47. Fradette N., Marsan B. (1998). Surface studies of $Cu_xCo_{3-x}O_4$ electrodes for the electrocatalysis of oxygen evolution, J. Electrochem. Soc., 145:2320-2327, https://doi.org/10.1149/1.1838637.
48. Singh R. N., Pandey J. P., Anitha K. L. (1993). Preparation of electrodeposited thin films of nickel-iron alloys on mild steel for alkaline water electrolysis. Part I: studies on oxygen evolution, Int. J. Hydrogen Energy, 18:467-473. https://doi.org/10.1016/0360-3199(93)90002-R
49. Singh N. K., Tiwari S. K., Anitha K. L., Singh R. N. (1996). Electrocatalytic properties of spinel-type $Mn_xFe_{3-x}O_4$ synthesized below 100°C for oxygen evolution in KOH solutions, J. Chem. Soc. Faraday Trans., 92(13):2397-2400. https://doi.org/10.1039/FT9969202397.
50. Wu Wei, Guo Shaoqiang, Zhang Jinsuo (2018). Electrochemical Behaviors of Cr(III) in Molten LiF-NaF-KF Eutectic, Int. J. Electrochem. Sci., 13:225-234. doi: 10.20964/2018.01.21.
51. Massot L., Chamelot P., Cassayre L., Taxil P. (2009). Electrochemical study of the Eu(III)/Eu(II) system in molten fluoride media, Electrochim Acta, 54:6361-6366. https://doi.org/10.1016/j.electacta.2009.06.016.
52. Bard A. J., Faulkner L. R. (2001). Electrochemical Methods: Principles and Applications, 2nd ed., Wiley, New York.
53. Gileadi E. (1993). Electrode Kinetics, (VCH Publishers Inc., New York), p.151.
54. Singh R. N., Pandey J. P., Singh N. K., Lal B., Chartier P., Koenig J. F. (2000). Sol-gel derived spinel $M_xCo_{3-x}O_4$ (M = Ni, Cu; $0 \leq x \leq 1$) films and oxygen evolution, Electrochim Acta, 45:1911-1919, https://doi.org/10.1016/S00134686 (99)00413-2